

Polyglutamine Aggregation Behavior *in vitro* Supports a Recruitment Mechanism of Cytotoxicity

Songming Chen, Valerie Berthelie, Wen Yang and Ronald Wetzel*

Graduate School of Medicine
University of Tennessee
Medical Center, 1924 Alcoa
Highway, Knoxville
TN 37920, USA

In expanded CAG repeat diseases such as Huntington's disease, proteins containing polyglutamine (poly(Gln)) sequences with repeat lengths of about 37 residues or more are associated with development of both disease symptoms and neuronal intranuclear inclusions (NIIs). Disease physiology in animal and cellular models does not always correlate with NII formation, however, and the mechanism by which aggregate formation might lead to cytotoxicity is unknown. To help evaluate various possible mechanisms, we determined the biophysical properties of a series of simple poly(Gln) peptides. The circular dichroism spectra of poly(Gln) peptides with repeat lengths of five, 15, 28 and 44 residues are all nearly identical and are consistent with a high degree of random coil structure, suggesting that the length-dependence of disease is not related to a conformational change in the monomeric states of expanded poly(Gln) sequences. In contrast, there is a dramatic increase in both the kinetics and the thermodynamic favorability of the spontaneous formation of ordered, amyloid-like aggregates for poly(Gln) peptides with repeat lengths of greater than 37 residues. At the same time, poly(Gln) peptides with repeat lengths in the 15–20 residue range, despite their poor abilities to support spontaneous, self-nucleated aggregation, are capable of efficiently adding to an already-formed aggregate. We also find that morphologically small, finely divided aggregates are much more efficient at recruiting poly(Gln) peptides than are large aggregates, suggesting a possible explanation for why disease pathology does not always correlate with the observable NII burden. Together, these data are consistent with a model for disease pathology in which critical cellular proteins possessing poly(Gln) sequences of modest length become inactivated when they are recruited into aggregates of an expanded poly(Gln) protein.

© 2001 Academic Press

Keywords: polyglutamine; aggregation; Huntington's disease; inclusion; nucleation

*Corresponding author

Introduction

Mutational expansion of CAG repeats in specific genes, with commensurate expansion of their encoded polyglutamine (poly(Gln)) sequences, is

responsible for at least eight neurodegenerative diseases, including Huntington's disease (HD).¹ In most of these diseases, poly(Gln) sequences with repeat lengths of up to about 35 residues are benign, while repeat lengths of 37 residues or greater are associated with disease.¹ Age of onset decreases, and disease severity and/or penetrance increases, with further increases in poly(Gln) length.² In the past four years, a number of laboratories have reported results from animal and cellular models showing that poly(Gln) transgene-dependent neurodegeneration is accompanied by the formation of 1–2 μm neuronal intranuclear inclusions (NIIs) staining for the expanded poly(Gln) protein.³ These findings are consistent with the observation of neuronal inclusions in

Abbreviations used: poly(Gln), polyglutamine; NII, neuronal intranuclear inclusions; HD, Huntington's disease; ThT, thioflavin T; C_c , critical concentration; CBP, CREB-binding protein; AT-3, ataxin-3; HPLC, high-performance liquid chromatography; TFA, trifluoroacetic acid; HFIP, hexafluoroisopropanol; PBS, phosphate-buffered saline; ELISA, enzyme-linked immunosorbent assay.

E-mail address of the corresponding author:
rwetzel@mc.utmck.edu

affected cells from HD brains.⁴ The role of protein aggregation in HD etiology has been controversial, however. Although NII appearance is well correlated with disease pathology in some models, in other experiments workers have observed either neurotoxicity without NII formation, or NII formation without neurotoxicity.⁵ Moreover, it is not clear how poly(Gln) aggregates might contribute to cell death and disease physiology.

According to one cytotoxicity hypothesis, aggregation of the poly(Gln) disease protein initiates a process of recruitment and sequestration of other poly(Gln)-containing cellular proteins into the growing aggregate, leading to their functional depletion from the local environment.^{6,7} Such a mechanism might be expected to be particularly effective when it involves proteins that operate in the cell at low concentrations and under tight regulation. In fact, a significant number of transcription factors contain poly(Gln) sequences,⁸ and alterations in transcriptional activity have been observed in poly(Gln) disease models.^{9–11} The possibility of cytotoxic consequences of co-aggregation between disease-related expanded poly(Gln) proteins like huntingtin and normal cellular poly(Gln) proteins introduces the question of the biophysical rules governing poly(Gln) aggregation and co-aggregation processes.

In contrast to the rapid advances made in cell and animal studies, we have only a rudimentary knowledge of many aspects of the fundamental physical properties of poly(Gln) sequences. Using recombinant protein fragments containing both poly(Gln) and other amino acid sequences, Wanker and colleagues have demonstrated a good correspondence between the length-dependence of spontaneous aggregation of poly(Gln) sequences *in vitro* and the length-dependence of disease risk.¹² In addition, several laboratories have published qualitative data showing that proteins containing poly(Gln) sequences of intermediate length can co-aggregate with poly(Gln) proteins of pathological length.^{6,13–18}

Here, we provide quantitative *in vitro* data on the aggregation of simple, well-defined poly(Gln) peptides lacking extensive additional sequence elements. The data add support to the recruitment-sequestration mechanism and better define the biophysical rules guiding aggregation and recruitment that might underlie poly(Gln) pathology. The data also suggest a reason for the incomplete correlation in cellular and animal model studies between NII formation and disease pathology.

Results

Previous efforts to investigate the fundamental folding behavior of simple, chemically synthesized poly(Gln) repeat sequences have been foiled by the high insolubility of peptides with repeat lengths greater than Q₁₅ to Q₂₀.^{19–21} Because of this, the only information we have on the biophysical beha-

avior of longer poly(Gln) peptides comes from studies involving transiently soluble proteolytic fragments of recombinant poly(Gln)-containing proteins.^{12,22} Recently, we devised a solvent treatment that renders poly(Gln) peptides up to repeat lengths of at least Q₄₄ transiently soluble in aqueous buffers.²³ This discovery makes it possible to focus on the intrinsic properties of the poly(Gln) sequence itself, both in studies of the conformational properties of these sequences in solution, and in aggregation studies.

Solution structure of poly(Gln) peptides

Figure 1 shows the circular dichroism (CD) spectra of freshly disaggregated poly(Gln) peptides with repeat lengths of Q₅, Q₁₅, Q₂₈, and Q₄₄ at neutral pH. All four spectra resemble the CD spectra of polypeptides in the random coil state.²⁴ The large negative molar ellipticities found for these peptides suggest that they exist in a statistical coil state under these conditions. The similar values of their molar ellipticities suggest that all four peptides, whether below or above the pathological cut-off length of 37 glutamine residues, populate the random coil conformation to the same extent. The large absolute values of these molar ellipticities, compared to the amplitudes typically seen for model random coil peptides (–10,000 to –40,000²⁵), suggest that random coil is the predominant state of these poly(Gln) peptides in solution. Details of the CD spectrum of the Q₅ peptide differ somewhat from those of the other three peptides. This may be due to a combination of the

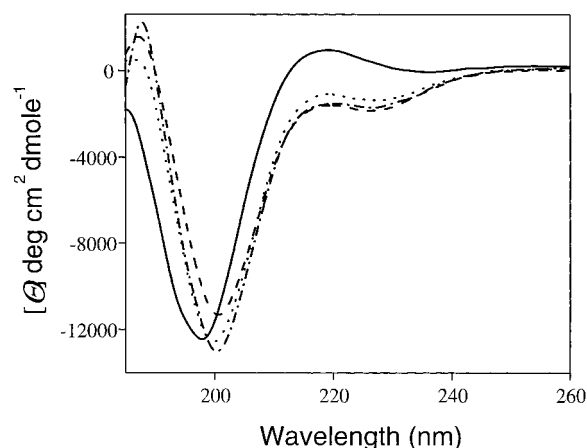


Figure 1. Circular dichroism spectra of 0.4 mg/ml solution of freshly disaggregated Q₅ (—), D₂Q₁₅K₂ (---), Q₂₈ (·····), and Q₄₄ (-·-·) peptides dissolved in filtered 10 mM Tris-trifluoroacetate (pH 7.0). Spectra were collected at 37°C on an OLIS DSM 1000 CD spectrophotometer in a 1-mm path-length quartz cuvette. The CD spectra, expressed in terms of mean residue weight ellipticity, represent the average of six spectral scans each. The small apparent difference in spectra at 190 nm is attributable to noise in the data due to light-absorption by the buffer in the far-UV region.

relatively short length (nine residues) of the Q₅ peptide, and the fact that in this peptide the Lys residues added to enhance peptide solubility constitute over 40% of the length of the peptide.

Previous studies found either random coil²⁰ or more ordered secondary structure²¹ in short poly(Gln) peptides. The results shown in Figure 1 suggest that soluble, monomeric forms of poly(Gln) do not adopt significant ordered secondary structure. It might be argued that, when dissolved in aqueous buffer after the organic solvent disaggregation treatment, these peptides may become kinetically trapped in a local free-energy minimum and therefore do not exhibit their most stable conformation. However, we incubated a long poly(Gln) peptide at 37°C and pH 7 for days, observing a slow transition from random coil to beta-sheet, which corresponds exactly to the kinetics of the monomer to aggregate transition (S. C. & R. W., unpublished results); we interpret this to indicate that the random coil state is the state thermodynamically favored by the monomer.

The comparison shown in Figure 1 suggests that there is no large structural difference between peptides shorter and longer than the pathological repeat length cutoff. Circular dichroism is a low-resolution technique, however, and it remains possible that length-dependent structural differences may exist that are not accompanied by large changes in the CD spectra.

Nucleation-dependent, homologous aggregation of poly(Gln) peptides

Figure 2 shows the time-dependent aggregation of a series of poly(Gln) peptides of different lengths. In these experiments, we monitored the aggregation reactions by following Rayleigh light-scattering increases over time. Similar data, with similar trends, were obtained using thioflavin T (ThT) fluorescence²⁶ to monitor aggregation (data not shown). Since ThT binding and fluorescence has been used to monitor amyloid fibril assembly,²⁶ this suggests that poly(Gln) aggregates may be related to amyloid fibrils at the molecular level. Such "amyloid-like" fibrillar morphology has been observed in aggregates formed *in vitro* from poly(Gln)-containing recombinant proteins,²² as well as simple synthetic peptides (S. C. & R. W., unpublished results). However, the degree to which poly(Gln) aggregates possess all aspects of classic amyloid structure²⁷ is yet to be established.

The kinetic behavior exhibited by these peptides is characteristic of a nucleation-dependent aggregation process, featuring a lag phase associated with organization of a nucleus and an extension phase associated with aggregate growth.²⁸⁻³⁰ Figure 2 shows that a Q₁₅ peptide displays little, if any, tendency to aggregate, exhibiting a lag time of more than 250 hours (in fact, the Q₁₅ peptide does eventually aggregate, but only after incubation for months at 37°C; S.C., unpublished results). Peptides containing 25-32 glutamine residues have lag

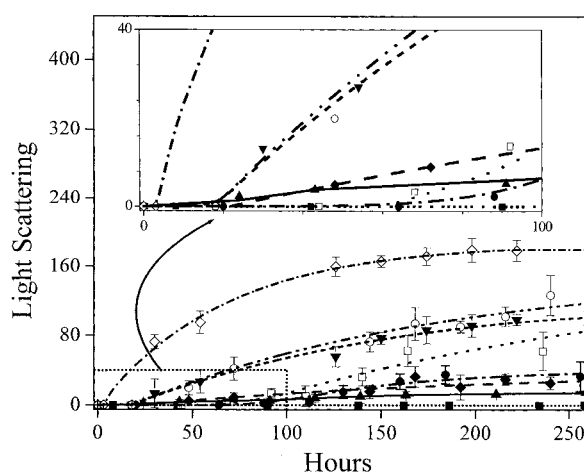


Figure 2. Solution phase growth of poly(Gln) aggregates. Poly(Gln) peptides Q₁₅ (■.....), Q₂₀ (▲—), Q₂₅ (●---), Q₂₈ (◆— — —), Q₃₂ (□.....), Q₃₇ (▼---), Q₄₁ (○---), and Q₄₄ (◇---) were disaggregated and incubated at 57 μg/ml in PBS at 37°C. Aggregation was monitored by light-scattering. In these experiments, we obtain essentially identical results using both thioflavin T and solubility assays based on reversed-phase HPLC chromatography. We obtained very similar results in a separate experiment using equal molar (10 μM) concentrations of each peptide. Inset is a blowup of kinetics curves between zero and 100 hours. Error bars reflect the standard deviation for two independent determinations for each datum point.

times in the range of 25-100 hours, and reactions proceed very slowly once aggregation is initiated. As poly(Gln) repeat length increases into the Q₃₇-Q₄₁ range, reactions exhibit lag times of around 20 hours and proceed more aggressively once initiated. The longest poly(Gln) peptide, with a repeat length of Q₄₄, experiences a lag phase of only a few hours (see inset, Figure 2) before it begins to aggregate very rapidly, with aggregation nearing completion after four to five days. It is formally possible that Q₄₄ exhibits such a short lag phase, because our rigorous disaggregation protocol (see Materials and Methods) did not completely remove aggregation seeds from the starting solution of monomer. At present we have no independent way to confirm the complete absence of aggregates from these poly(Gln) solutions. However, we do not think it is likely that Q₄₄ is uniquely contaminated by residual seeds; the behavior of Q₄₄ is consistent with the general trend in the data of shorter lag phases for longer poly(Gln) sequences. Further, an exact repeat of the spontaneous aggregation kinetics for the Q₃₇ peptide, shown in Figure 3 as part of the seeding experiment, gives very similar data to that shown in Figure 2. The most likely way to achieve reproducible kinetics would be if in the preparation of solubilized monomer one obtained reproducible elimination of seeds, rather than reproducible retention of a similar residual seed content.

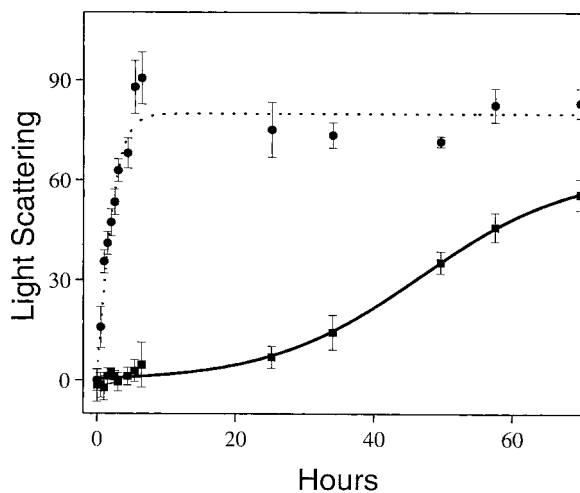


Figure 3. Effect of added aggregation seed on lag time. Seed was prepared by aggregation of the Q₃₇ peptide at -20°C , followed by concentration to 1.5 mg/ml by centrifugation at 20,800 g for 30 minutes, and sonication with a probe sonicator for three minutes at 0°C . Disaggregated Q₃₇ peptide (57 $\mu\text{g}/\text{ml}$; 10 μM) was incubated in PBS at 37°C either without (■—) or with (○·····) 5% (w/w) of the Q₃₇ seed. The data were fit to sigmoidal curves. Error bars show the standard deviation of two independent measurements.

Figure 2 suggests that the repeat length-dependence of disease risk may be related to the repeat length-dependence of nucleation kinetics. Similar trends have been observed in an analysis of proteolytic fragments of recombinant poly(Gln) proteins.¹²

Another feature of nucleated growth pathway is the ability of added aggregates to abort the lag phase of an aggregation reaction by seeding growth.³⁰ Figure 3 shows that seeding is observed in a solution phase aggregation reaction spiked with preformed aggregates. In the experiment shown, added poly(Gln) aggregates equivalent to 5% by weight of the soluble monomer completely eliminate the lag phase observed in the absence of added seed. These results are similar to those observed in A β fibril formation reactions.³¹

Another parameter that characterizes polymerization reactions is the critical concentration (C_r). The C_r is the concentration of monomer remaining when a polymerization reaction reaches equilibrium, and is thus related to the equilibrium constant between monomer and aggregate.^{28,30} Thus, while the nucleation lag time is a kinetic parameter, the C_r value describes the thermodynamic favorability of a polymerization reaction and the likelihood it will occur at a particular monomer concentration. By measuring residual levels of non-aggregated peptides in aggregation reactions using HPLC or other methods (see Materials and Methods), we determined approximate C_r values for poly(Gln) aggregation and found that these C_r

values also display a significant repeat length-dependence. For example, we obtained C_r in the range of 30 μM for the Q₁₅ peptide, while the C_r for the Q₂₀ peptide drops about an order of magnitude into the 3–4 μM range. The Q₄₄ peptide exhibits a C_r of about 70 nM. These values indicate that as poly(Gln) repeat length goes up, polymerization becomes more thermodynamically favorable and therefore can occur at lower poly(Gln) concentrations.

The steady-state cellular levels of soluble poly(Gln) disease-related proteins are not known. If the cellular concentration of huntingtin, the poly(Gln) protein responsible for HD, is normally less than 1 μM , this would suggest that an expansion of the poly(Gln) sequence from Q₂₀ to Q₄₄ would correspond to a change in the thermodynamics of aggregation from unfavorable to favorable. For those proteins containing poly(Gln) sequences for which aggregation is thermodynamically allowed at cellular protein concentrations, the length-dependence of nucleation similar to that shown in Figure 2 presumably controls how aggressively the protein aggregates. The length-dependence of the C_r and the nucleation phase may thus together be responsible for the strong inverse correlation between repeat length and age-of-onset² in these diseases.

Heterologous extension of poly(Gln) peptides

Light-scattering and ThT fluorescence are measures responding to the total mass of an aggregate, and therefore are limited in their ability to provide detailed quantification of heterologous aggregation reactions. To explore the recruitment hypothesis of aggregate cytotoxicity, we wanted to be able to specifically monitor the repeat length-dependence of heterologous aggregate extension; that is, the ability of one poly(Gln) peptide to assemble into an aggregate of another poly(Gln) peptide. To do this, we devised a microtiter plate assay in which aggregates of one length of poly(Gln) are fixed to the microplate well, then incubated with another length of poly(Gln) that is tagged to allow monitoring of its deposition onto the fixed aggregates. In the experiments described here, the tag is a biotin moiety at the N terminus of the poly(Gln) peptide, which is then monitored by complexation with europium-streptavidin, followed by quantification using time-resolved fluorescence.³²

As shown in Figure 4(a), biotinylated poly(Gln) peptides of different lengths are readily deposited onto immobilized Q₃₇ poly(Gln) aggregates. Interestingly, the extension reaction displays two-phase kinetics, very similar to what is observed in the homologous extension of A β amyloid fibrils in a similar microtiter plate assay.³³ Figure 4(a) shows that both the amplitude and the rate of the initial, rapid phase of the extension reaction increase with increasing poly(Gln) repeat length. Peptides with repeat lengths of Q₅–Q₁₀ exhibit only a small

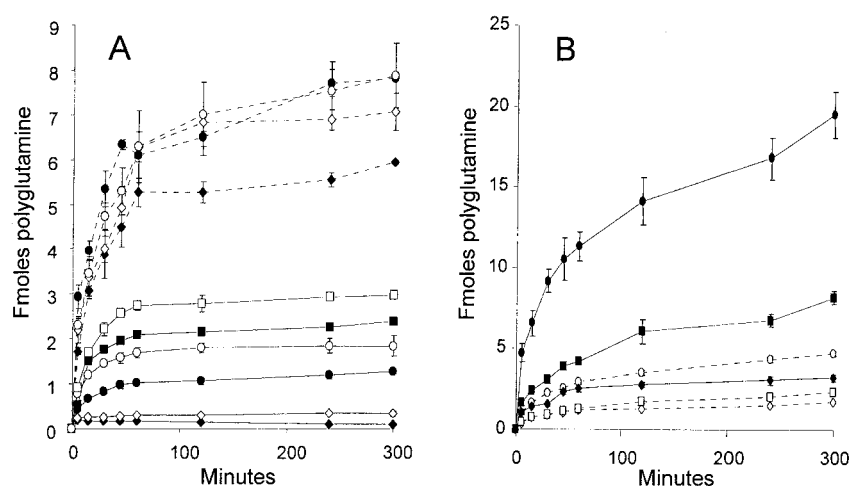


Figure 4. Extension of poly(Gln) aggregates by tagged monomeric poly(Gln) peptides. (a) Q_{37} aggregates of type of the type shown in Figure 5(b) were fixed to the plate and biotinyl-poly(Gln) peptides of various lengths incubated as described. The different lengths of peptides used were (—◆—) Q_5 , (—◇—) Q_{10} , (—●—) Q_{15} , (—○—) Q_{20} , (—■—) Q_{25} , (—□—) Q_{28} , (··◆··) Q_{35} , (··◇··) Q_{39} , (··●··) Q_{44} and (··○··) Q_{49} . (b) Biotinyl- Q_{28} (10 nM) was incubated in microplate wells with 80 ng of Q_{37} aggregates growth at 37°C (··◇··) and sonicated (··□··) and filtered (··○··) or Q_{37} aggregates formed by incubation at -20°C (—◆—) and sonicated (—■—) and filtered (—●—).

degree of binding/extension under these conditions. In contrast, peptides with repeat lengths of Q_{15} or Q_{20} can readily add to pre-existing aggregates under these conditions. As the poly(Gln) repeat length further increases up to Q_{39} , the ability to be recruited also increases. Further length increases, represented by the Q_{44} and Q_{49} peptides, do not add measurably to the rate of extension. These data suggest that, while poly(Gln) repeat length also contributes to extension activity, length constraints are less severe for aggregate extension than for spontaneous nucleation. In particular, these data show that peptide elements as short as Q_{15} are sufficient to support the recruitment of a poly(Gln)-containing protein by a pre-existing aggregate.

Dependence of recruitment on poly(Gln) aggregate morphology

Our ability to exert some control over poly(Gln) solubility and aggregate growth also provides an opportunity to study the properties of poly(Gln) aggregates. A number of aggregate morphologies from *in vitro* assembly of poly(Gln) proteins and peptides have been reported, including small curvilinear filaments,¹⁹ broad ribbons,²² and amyloid-like fibrils.¹² Figure 5 shows the morphologies of two aggregated states we produced *in vitro* from the same synthetic poly(Gln) Q_{37} peptide. The broad ribbon morphology shown in Figure 5(a) is similar to structures observed in the aggregation of proteolytic fragments of the N-terminal domain of huntingtin containing a Q_{51} repeat.²² These broad ribbons of about 50 nm in width and 500 nm or more in length appear in the electron microscope to consist of a sub-structure of aligned, straight filaments. The thin filaments shown in Figure 5(b)

resemble previously observed small aggregates of a Q_{15} peptide,¹⁹ and are similar to the protofibrillar intermediates in $A\beta$ aggregation *in vitro*.³⁴ These filaments, 3–4 nm in diameter and about 50 nm in length, appear similar in diameter to the filamentous components of the ribbons shown in Figure 5(a).

Figure 4(b) shows that different aggregated states of the same poly(Gln) sequence exhibit dramatically different abilities to serve as templates for heterologous extension by other poly(Gln) peptides. We prepared six different versions of aggregates of the Q_{37} peptide. One series was prepared by incubating peptide at 37°C to generate the large, ordered aggregates shown in Figure 5(a). The other series was prepared from aggregates assembled in a reaction at -20°C , like those shown in Figure 5(b). In both cases, sub-populations of aggregates were also prepared, by sonication either with or without a following membrane filtration step. For each of the six resulting aggregate preparations, the weight concentration of aggregates was determined and equal weights of aggregates were fixed to the wells of microtiter plates.

Figure 4(b) shows that these aggregates, all derived from the same Q_{37} peptide, vary considerably in their weight-normalized abilities to support heterologous extension by a biotinylated Q_{28} peptide. Two trends are readily apparent. First, filamentous -20°C aggregates are more efficient in supporting extension than are the broad ribbons generated at 37°C. Secondly, within each of these two series, smaller particles are more efficient at supporting extension than are larger ones (sonicated + filtered > sonicated > non-sonicated). The results suggest that the ability of an aggregate to support extension may depend, in part, on its

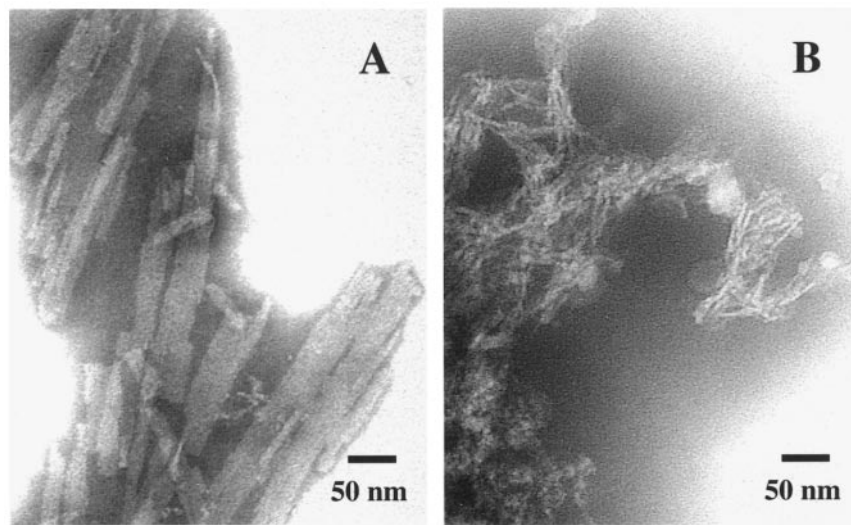


Figure 5. Aggregates of the Q₃₇ peptide prepared as described were fixed to mica grids and negatively stained with a 0.25% (w/v) potassium phosphotungstate solution, and analyzed by transmission electron microscopy on a Hitachi H-600 electron microscope. (a) Aggregates grown at 37°C. (b) Aggregates formed by incubation at -20°C.

“extension-competent” surface area. The results also suggest, however, that fine structure within the aggregate, as manifested by the filamentous *versus* ribbon morphology in the electron microscope, may also impart some differences in the intrinsic extension efficiencies of different forms. The data shown in Figure 4(b) correspond to a 20-fold difference in initial extension rate between the smallest (sonicated and filtered, -20°C aggregate) and the largest (non-sonicated, 37°C aggregate) aggregates tested, showing that aggregate size and morphology together have a significant influence on extension efficiency.

Discussion

Deposition of protein aggregates is an aspect of the pathology of a growing number of neurodegenerative diseases, including Alzheimer’s disease, Parkinson’s disease, prion diseases, amyotrophic lateral sclerosis, and expanded CAG repeat diseases like HD.³⁵ Several systemic amyloidoses also sometimes manifest as peripheral neuropathies.³⁶ The mechanisms by which these protein aggregates disrupt normal cell function and ultimately lead to cell death and tissue atrophy are unknown. One mechanism that has received relatively little attention is the recruitment/sequestration model, in which molecules carrying out important functions at low concentration are drawn into growing protein aggregates, thereby depriving the local cellular environment of their function and inducing cellular stress. In addition to the expanded poly(Gln) repeat diseases, mechanisms of cytotoxicity related to this heterologous recruitment-sequestration mechanism have been considered in discussions of Alzheimer’s disease,^{37,38} Parkinson’s disease,³⁹ and amyotrophic lateral sclerosis.⁴⁰ In addition, efficient homologous recruitment of certain proteins into

inactive aggregates is the basis for the loss of function phenotypes at the core of the yeast prion phenomenon.⁴¹

The recruitment/sequestration model is particularly attractive in the case of the expanded poly(Gln) diseases. In these diseases, there is a clear, structurally attractive molecular mechanism that might potentially endow the recruitment process with a degree of specificity, the shared poly(Gln) sequences of the proteins involved. Many of the poly(Gln) proteins found in the genome database are transcription factors of one kind or another, acting in the nucleus at low, tightly regulated concentrations. Most (but not all) poly(Gln) inclusions are observed to reside in cell nuclei, and transcription dysfunction is a common attribute of poly(Gln) pathology.¹¹ Two of the proteins for which expansion of a poly(Gln) track is associated with neurodegeneration, TBP⁴² and the androgen receptor,⁴³ are themselves transcription factors.

That two poly(Gln)-containing proteins might be capable of co-aggregating *in vivo* was suggested by the observation of recruitment of full-length ataxin-3 (AT-3) into aggregates of an AT-3 fragment containing an expanded CAG repeat.¹³ Normal, wild-type poly(Gln)-containing proteins that are not known to aggregate independently *in vivo* have been shown to co-localize to aggregates of expanded poly(Gln) proteins in various disease models.^{6,14-18} Particularly striking are recent experiments showing the interactions between aggregates of expanded poly(Gln) proteins and the transcription factor CREB-binding protein (CBP). Transfected cells containing cytotoxic N11s formed from expanded poly(Gln) repeat proteins exhibit both co-localization of CBP to nuclear aggregates¹⁶⁻¹⁸ and loss of CBP protein¹⁷ and CBP-related transcriptional activity¹⁸ from the soluble

fraction. In contrast, neither a Q₁₉-deleted form of CBP, nor P300, a CBP homolog containing only a Q₆ repeat, are recruited into NIIs.¹⁸ While expression of expanded poly(Gln) protein is toxic to these cells, cytotoxicity is reversed by overexpression of various forms of CBP.^{17,18}

The analysis of poly(Gln) aggregation reported here is consistent with a number of the details of the recruitment/sequestration mechanism. First, we observe little apparent secondary structure difference between short and long poly(Gln) peptides in their circular dichroism spectra, arguing against mechanisms of cytotoxicity based on length-dependent conformational changes at the level of the soluble monomer. Second, we observe a strong length-dependence to the critical concentrations and aggregation lag times of simple poly(Gln) peptides in their nucleation-dependent aggregation, suggesting that the poly(Gln) length-dependence of disease risk may be linked to nucleated aggregation within the cell. Third, we find that, once aggregation is initiated by a longer poly(Gln) sequence, poly(Gln) peptides in the Q₁₅-Q₂₀ range are recruited into the growing aggregate efficiently, while Q₅ or Q₁₀ peptides are recruited much less efficiently (Figure 4(a)). These results are consistent with the observation that a Q₁₉ protein, CBP, is recruited into cellular poly(Gln) aggregates,¹⁶⁻¹⁸ while its Q₆ homolog, P300, is not.¹⁸

Finally, our observation of an inverse relationship between the size and recruitment activity (Figure 4(b)) of different forms of aggregates may help to explain the inability of some animal and cellular models to demonstrate good correlations between NII formation and cytotoxicity. In many of these experiments, diffuse nuclear staining as detected by fluorescence microscopy is often equated with a "soluble" state of the poly(Gln) protein, while the formation of large (>1 μm) NIIs is considered to be an accurate reporter of the transition to an "aggregated" state. In contrast, when (higher resolution) electron microscopy is used to analyze the substructures of NIIs from HD patients⁴ and from mouse models,²² it reveals within the NII a series of punctate and filamentous aggregates whose sizes are more in the range of the *in vitro* filaments shown in Figure 4(b). Importantly, small immunostaining filaments can also be seen on the periphery of the NIIs in the electron micrographs,^{4,44} suggesting the possibility of the independent existence of small poly(Gln) aggregates within the cell. The results shown in Figure 4(b) suggest that the recruitment-associated activity of poly(Gln) aggregates in the cell may also decrease as their size (and hence their visibility in fluorescence light microscopy) increases. The implication that not all poly(Gln) aggregates are equally important is reminiscent of data assigning special biological significance to small aggregated forms of Aβ⁴⁵⁻⁴⁹ as well as theoretical treatments of the importance of aggregate size on prion infectivity.⁵⁰ Together with the present report, these recent con-

tributions reaffirm the importance of recognizing the existence of multiple protein aggregated states in modeling protein-folding diseases.⁵¹

The *in vivo* relevance of the morphological forms reported here for aggregates of chemically synthesized poly(Gln) peptides is not known. As discussed above, both ribbons and fibrils have been described for *in vitro* aggregates of poly(Gln)-containing disease-related proteins, and both isolated and clumped filamentous aggregates are observed in cells. Whether or not the *in vitro* filaments reported here are relevant to poly(Gln) pathology, the inverse correlation we observe here between aggregate size and recruitment activity is likely to be germane to whatever poly(Gln) aggregates are formed in the cell.

The data reported here suggest that, while poly(Gln) sequences must reach a repeat length of about Q₃₇ or higher to promote efficient nucleation-dependent aggregation, proteins with poly(Gln) repeats as low as Q₁₅-Q₂₀ should be susceptible to being recruited into aggregates once the process is initiated. Our *in vitro* observation of a class of small, ordered aggregates capable of promoting aggressive poly(Gln) recruitment suggests that surveys limited to large, easily detectable aggregates may not give an accurate picture of poly(Gln)-related cytotoxic activity within a cell. A better measure of the disease-related impact of the aggregate burden of a cell or tissue may be the recruitment activity associated with those aggregates. Derivative versions of the microplate assay utilized here should prove valuable both in quantifying this recruitment activity in biological samples and in screening compound libraries for potential inhibitors of poly(Gln) aggregation and/or aggregate extension.

Materials and Methods

Materials and basic methods

Peptides were obtained by custom solid-phase synthesis from the Keck Biotechnology Center at Yale University. Synthetic peptides had a common sequence context of a poly(Gln) sequence flanked by pairs of lysine residues: K₂Q_{*n*}K₂. The Lys residues are added to confer a net positive charge on the peptides at pH 7 to enhance solubility; in fact, a Q₃₇ peptide lacking the flanking Lys residues and subjected to the standard disaggregation protocol (see below) exhibits instantaneous aggregation at both pH 3 and pH 7 (S. C., unpublished results). For the microplate extension assay, peptides were obtained in which a biotin group was appended to the α-amino group of the N-terminal Lys residue of the completed peptide product. Light-scattering measurements were conducted on aliquots of aggregation reactions transferred to a fluorescence cuvet and read as apparent fluorescence in a Perkin-Elmer LS50B fluorometer with emission and excitation wavelengths both set at 450 nm, and with the emission and excitation slit-widths both set at 2 nm. Approximate critical concentration values were obtained by allowing an aggregation reaction to reach equilibrium, then quantifying the amount of unpolymerized material by either the A₂₂₀

absorbance peak in reverse phase HPLC (compared to a poly(Gln) peptide standard characterized by amino acid composition analysis; Commonwealth Biotechnologies, Inc.) or the fluorescence of a fluorescein-tagged version of the peptide (also obtained from the Keck Center).

Disaggregation of poly(Gln) peptides

Details of the solubilization protocol, which is derived from a method previously described for disaggregation of the Alzheimer's peptide A β ,⁵² are as described.²³ Briefly, lyophilized synthetic peptides were suspended in a mixture of trifluoroacetic acid (TFA) and hexafluoroisopropanol (HFIP) and incubated at room temperature to insure complete dissolution. The volatile solvent mixture was removed under a stream of argon, the peptide residue dissolved in water adjusted to pH 3 with TFA, and the resulting solution further disaggregated by ultracentrifugation. Aggregation reactions were initiated by addition of a phosphate-buffered saline (PBS) buffer concentrate.

Growth of aggregates in solution phase

Peptides were disaggregated as described above. Disaggregated peptides were adjusted to a concentration of 57 μ g/ml in PBS and incubated at 37°C to produce the kinetics shown in Figure 2. The aggregates shown in Figure 5(a) were grown at 37°C at a poly(Gln) concentration of 10 μ M. For the assay summarized in Figure 4(a), and for the aggregates shown in Figure 5(b), peptides were incubated in PBS at 37°C, then snap frozen and further incubated at -20°C. For the kinetic data shown in Figure 4(b), some aggregates were further processed by sonication with a probe sonicator (two minutes at 0°C) followed by filtration through a 1.22 μ m membrane filter. The mechanism by which aggregation conditions control aggregate morphology is at present unknown. A description of the factors influencing aggregation at -20°C will be described elsewhere (B. Hamilton and R. W., unpublished results).

Microtiter plate extension reaction

Aggregates (80 ng per well) prepared as described above, were fixed to activated enzyme-linked immunosorbent assay (ELISA) microtiter plates by overnight incubation followed by washing with assay buffer consisting of 0.01% (w/v) Tween-20 and 0.05% (w/v) sodium azide in PBS. In the experiment shown in Figure 4(b), quantitative attachment of the aggregates to the microplate wells was confirmed by recovery of the supernatant from the wells after the fixation step, centrifugation to recover any non-fixed aggregate, addition of TFA to solubilize any non-fixed aggregate, and injection of the diluted TFA extract onto the high performance liquid chromatography (HPLC). Essentially no poly(Gln) was recovered, in contrast to standard suspensions of aggregate treated similarly.

Solutions (10 nM) of disaggregated biotinyl-poly(Gln) peptides were incubated at 37°C for various times in aggregate-containing wells. These supernatants were then discarded and the wells washed and incubated at room temperature with a solution of a europium complex of streptavidin (EG&G Wallac). Wells were washed and the deposited europium released into solution with a complexation buffer (EG&G Wallac Enhancement Buffer), then counted by time-resolved fluorescence in a

Victor 2 1420 multilabel counter (EG&G Wallac). Details of the assay reported elsewhere are.^{53,54}

Acknowledgments

R.W. acknowledges support from the Lindsay Young Gift Fund, and from the Hereditary Disease Foundation in the form of a Lieberman Award and a Cure Huntington's Disease Initiative contract. We thank Brad Hamilton for preparation of aggregates, Angela Williams for HPLC purification of poly(Gln) peptides, Charles Murphy for mass spectrometric analysis of poly(Gln) peptides, and Jonathan Wall for helpful discussions.

References

- Cummings, C. J. & Zoghbi, H. Y. (2000). Fourteen and counting: unraveling trinucleotide repeat diseases. *Hum. Mol. Genet.* **9**, 909-916.
- Myers, R. H., Marans, K. S. & MacDonald, M. E. (1998). Huntington's disease. In *Genetic Instabilities and Hereditary Neurological Diseases* (Wells, R. D. & Warren, S. T., eds), pp. 301-323, Academic Press, San Diego.
- Reddy, P. H., Williams, M. & Tagle, D. A. (1999). Recent advances in understanding the pathogenesis of Huntington's disease. *Trends Neurosci.* **22**, 248-255.
- DiFiglia, M., Sapp, E., Chase, K. O., Davies, S. W., Bates, G. P., Vonsattel, J. P. & Aronin, N. (1997). Aggregation of huntingtin in neuronal intranuclear inclusions and dystrophic neurites in brain. *Science*, **277**, 1990-1993.
- Zoghbi, H. Y. & Orr, H. T. (1999). Polyglutamine diseases: protein cleavage and aggregation. *Curr. Opin. Neurobiol.* **9**, 566-570.
- Perez, M. K., Paulson, H. L., Pendse, S. J., Saionz, S. J., Bonini, N. M. & Pittman, R. N. (1998). Recruitment and the role of nuclear localization in polyglutamine-mediated aggregation. *J. Cell. Biol.* **143**, 1457-1470.
- Preisinger, E., Jordan, B. M., Kazantsev, A. & Housman, D. (1999). Evidence for a recruitment and sequestration mechanism in Huntington's disease. *Philos. Trans. Roy. Soc. ser. B*, **354**, 1029-1034.
- Perutz, M. F. (1996). Glutamine repeats and inherited neurodegenerative diseases: molecular aspects. *Curr. Opin. Struct. Biol.* **6**, 848-858.
- Li, S. H., Cheng, A. L., Li, H. & Li, X. J. (1999). Cellular defects and altered gene expression in PC12 cells stably expressing mutant huntingtin. *J. Neurosci.* **19**, 5159-5172.
- Lin, X., Antalffy, B., Kang, D., Orr, H. T. & Zoghbi, H. Y. (2000). Polyglutamine expansion down-regulates specific neuronal genes before pathologic changes in SCA1. *Nature Neurosci.* **3**, 157-163.
- Cha, J. H. (2000). Transcriptional dysregulation in Huntington's disease. *Trends Neurosci.* **23**, 387-392.
- Scherzinger, E., Sittler, A., Schweiger, K., Heiser, V., Lurz, R., Hasenbank, R. et al. (1999). Self-assembly of polyglutamine-containing huntingtin fragments into amyloid-like fibrils: implications for Huntington's disease pathology. *Proc. Natl Acad. Sci. USA*, **96**, 4604-4609.
- Paulson, H. L., Perez, M. K., Trotter, Y., Trojanowski, J. Q., Subramony, S. H., Das, S. S. et al.

- (1997). Intranuclear inclusions of expanded polyglutamine protein in spinocerebellar ataxia type 3. *Neuron*, **19**, 333-344.
14. Huang, C. C., Faber, P. W., Persichetti, F., Mittal, V., Vonsattel, J. P., MacDonald, M. E. *et al.* (1998). Amyloid formation by mutant huntingtin: threshold, progressivity and recruitment of normal polyglutamine proteins. *Somat. Cell Mol. Genet.* **24**, 217-233.
 15. Kazantsev, A., Preisinger, E., Dranovsky, A., Goldgaber, D. & Housman, D. (1999). Insoluble detergent-resistant aggregates form between pathological and nonpathological lengths of polyglutamine in mammalian cells. *Proc. Natl Acad. Sci. USA*, **96**, 11404-11409.
 16. Steffan, J. S., Kazantsev, A., Spasic-Boskovic, O., Greenwald, M., Zhu, Y. Z., Gohler, H. *et al.* (2000). The Huntington's disease protein interacts with p53 and CREB-binding protein and represses transcription. *Proc. Natl Acad. Sci. USA*, **97**, 6763-6768.
 17. McCampbell, A., Taylor, J. P., Taye, A. A., Robitschek, J., Li, M., Walcott, J. *et al.* (2000). CREB-binding protein sequestration by expanded polyglutamine. *Hum. Mol. Genet.* **9**, 2197-2202.
 18. Nucifora, F. C., Jr., Sasaki, M., Peters, M. F., Huang, H., Cooper, J. K., Yamada, M. *et al.* (2001). Interference by huntingtin and atrophin-1 with cbp-mediated transcription leading to cellular toxicity. *Science*, **291**, 2423-2428.
 19. Perutz, M. F., Johnson, T., Suzuki, M. & Finch, J. T. (1994). Glutamine repeats as polar zippers: their possible role in inherited neurodegenerative diseases. *Proc. Natl Acad. Sci. USA*, **91**, 5355-5358.
 20. Altschuler, E. L., Hud, N. V., Mazrimas, J. A. & Rupp, B. (1997). Random coil conformation for extended polyglutamine stretches in aqueous soluble monomeric peptides. *J. Pept. Res.* **50**, 73-75.
 21. Sharma, D., Sharma, S., Pasha, S. & Brahmachari, S. K. (1999). Peptide models for inherited neurodegenerative disorders: conformation and aggregation properties of long polyglutamine peptides with and without interruptions. *FEBS Letters*, **456**, 181-185.
 22. Scherzinger, E., Lurz, R., Turmaine, M., Mangiarini, L., Hollenbach, B., Hasenbank, R. *et al.* (1997). Huntingtin-encoded polyglutamine expansions form amyloid-like protein aggregates *in vitro* and *in vivo*. *Cell*, **90**, 549-558.
 23. Chen, S. & Wetzel, R. (2000). Solubilization and disaggregation of polyglutamine peptides. *Protein Sci.* **10**, 887-891.
 24. Tilstra, L. & Mattice, W. L. (1996). The β sheet-coil transition of polypeptides, as determined by circular dichroism. In *Circular Dichroism and the Conformational Analysis of Macromolecules* (Fasman, G. D., ed.), pp. 261-283, Plenum, New York.
 25. Woody, R. W. (1996). Theory of circular dichroism of proteins. In *Circular Dichroism and Conformational Analysis of Biomolecules* (Fasman, G. D., ed.), pp. 25-67, Plenum, New York.
 26. LeVine, H. (1999). Quantification of β -sheet amyloid fibril structures with thioflavin T. In *Amyloid, Prions and other Protein Aggregates* (Wetzel, R., ed.), vol. 309, pp. 274-284, Academic Press, San Diego.
 27. Sipe, J. D. (1992). Amyloidosis. *Annu. Rev. Biochem.* **61**, 947-975.
 28. Timasheff, S. N. (1981). The self-assembly of long rodlike structures. In *Protein-Protein Interactions* (Frieden, C. & Nichol, L. W., eds), pp. 315-336, Wiley-Interscience, New York.
 29. Bishop, M. F. & Ferrone, F. A. (1984). Kinetics of nucleation-controlled polymerization. A perturbation treatment for use with a secondary pathway. *Biophys. J.* **46**, 631-644.
 30. Harper, J. D. & Lansbury, P. T., Jr (1997). Models of amyloid seeding in Alzheimer's disease and scrapie: mechanistic truths and physiological consequences of the time-dependent solubility of amyloid proteins. *Annu. Rev. Biochem.* **66**, 385-407.
 31. Wood, S. J., Chan, W. & Wetzel, R. (1996). Seeding of A β fibril formation is inhibited by all three isotypes of apolipoprotein E. *Biochemistry*, **35**, 12623-12628.
 32. Diamandis, E. P. (1988). Immunoassays with time-resolved fluorescence spectroscopy: principles and applications. *Clin. Biochem.* **21**, 139-150.
 33. Esler, W. P., Stimson, E. R., Jennings, J. M., Vinters, H. V., Ghilardi, J. R., Lee, J. P. *et al.* (2000). Alzheimer's disease amyloid propagation by a template-dependent dock-lock mechanism. *Biochemistry*, **39**, 6288-6295.
 34. Harper, J. D., Wong, S. S., Lieber, C. M. & Lansbury, P. T. (1997). Observation of metastable A β amyloid protofibrils by atomic force microscopy. *Chem. Biol.* **4**, 119-125.
 35. Martin, J. B. (1999). Molecular basis of the neurodegenerative disorders [published erratum appears in *N. Engl. J. Med.* (1999); **341**, 1407]. *N. Engl. J. Med.* **340**, 1970-1980.
 36. Falk, R. H., Comenzo, R. L. & Skinner, M. (1997). The systemic amyloidoses. *N. Engl. J. Med.* **337**, 898-909.
 37. Selkoe, D. J. (1994). Normal and abnormal biology of the β -amyloid precursor protein. *Annu. Rev. Neurosci.* **17**, 489-517.
 38. Wetzel, R. (1997). The role of accessory proteins in protein folding diseases. In *Molecular Chaperones in Proteins: Structure, Function, and Mode of Action* (Fink, A. & Goto, Y., eds), pp. 577-613, Marcel Dekker, New York.
 39. Nussbaum, R. L. (1998). Putting the parkin into Parkinson's. *Nature*, **392**, 544-545.
 40. Bruijn, L. I., Houseweart, M. K., Kato, S., Anderson, K. L., Anderson, S. D., Ohama, E. *et al.* (1998). Aggregation and motor neuron toxicity of an ALS-linked SOD1 mutant independent from wild-type SOD1. *Science*, **281**, 1851-1854.
 41. Lindquist, S. (1997). Mad cows meet psi-chotic yeast: the expansion of the prion hypothesis. *Cell*, **89**, 495-498.
 42. Koide, R., Kobayashi, S., Shimohata, T., Ikeuchi, T., Maruyama, M., Saito, M. *et al.* (1999). A neurological disease caused by an expanded CAG trinucleotide repeat in the TATA-binding protein gene: a new polyglutamine disease? *Hum. Mol. Genet.* **8**, 2047-2053.
 43. Merry, D. E. & Fischbeck, K. H. (1998). Genetics and molecular biology of the androgen receptor CAG repeat. In *Genetic Instabilities and Hereditary Neurological Diseases* (Wells, R. D. & Warren, S. T., eds), pp. 101-111, Academic Press, San Diego.
 44. Davies, S. W., Turmaine, M., Cozens, B. A., DiFiglia, M., Sharp, A. H., Ross, C. A. *et al.* (1997). Formation of neuronal intranuclear inclusions underlies the neurological dysfunction in mice transgenic for the HD mutation. *Cell*, **90**, 537-548.
 45. Lambert, M. P., Barlow, A. K., Chromy, B. A., Edwards, C., Freed, R., Liosatos, M. *et al.* (1998). Diffusible, nonfibrillar ligands derived from

- Abeta1-42 are potent central nervous system neurotoxins. *Proc. Natl Acad. Sci. USA*, **95**, 6448-6453.
46. Wilson, C. A., Doms, R. W. & Lee, V. M. (1999). Intracellular APP processing and A beta production in Alzheimer disease. *J. Neuropathol. Exp. Neurol.* **58**, 787-794.
47. Yang, A. J., Chandswangbhuvana, D., Shu, T., Henschen, A. & Glabe, C. G. (1999). Intracellular accumulation of insoluble, newly synthesized abeta-42 in amyloid precursor protein-transfected cells that have been treated with Abeta1-42. *J. Biol. Chem.* **274**, 20650-20656.
48. Guerette, R. A., Legg, J. T., Cherny, R. A., Mclean, C. A., Masters, C. L., Beyreuther, K. & Bush, A. I. (1999). Oligomeric Abeta in PBS-soluble extracts of human Alzheimer brain. *Abstr. 29th Annu. Meet. Soc. Neurosci.* **25**, 2129.
49. Walsh, D. M., Hartley, D. M., Kusumoto, Y., Fezoui, Y., Condron, M. M., Lomakin, A. *et al.* (1999). Amyloid beta-protein fibrillogenesis. Structure and biological activity of protofibrillar intermediates. *J. Biol. Chem.* **274**, 25945-25952.
50. Masel, J., Jansen, V. A. & Nowak, M. A. (1999). Quantifying the kinetic parameters of prion replication. *Biophys. Chem.* **77**, 139-152.
51. Wetzel, R. (1996). For protein misassembly, it's the "I" decade. *Cell*, **86**, 699-702.
52. Zagorski, M. G., Yang, J., Shao, H., Ma, K., Zeng, H. & Hong, A. (1999). Methodological and chemical factors affecting amyloid- β amyloidogenicity. In *Amyloid, Prions and other Protein Aggregates* (Wetzel, R., ed.), vol. 309, pp. 189-204, Academic Press, San Diego.
53. Berthelie, V., Hamilton, J. B., Chen, S. & Wetzel, R. (2001). A microtiter plate assay for polyglutamine aggregate extension. *Anal. Biochem.* **296**, in the press.
54. Berthelie, V. & Wetzel, R. (2002). An assay for characterizing the *in vitro* kinetics of polyglutamine aggregation. In *Methods in Molecular Medicine: Neurogenetics* (Potter, N., ed.), Humana Press, New York, in the press.

Edited by F. Cohen

(Received 16 February 2001; received in revised form 3 May 2001; accepted 11 June 2001)